Photochemical & Photobiological Sciences

Accepted Manuscript

This is an *Accepted Manuscript*, which has been through the Royal Society of Chemistry peer review process and has been accepted for publication.

Accepted Manuscripts are published online shortly after acceptance, before technical editing, formatting and proof reading. Using this free service, authors can make their results available to the community, in citable form, before we publish the edited article. We will replace this *Accepted Manuscript* with the edited and formatted *Advance Article* as soon as it is available.

You can find more information about *Accepted Manuscripts* in the Information for Authors.

Please note that technical editing may introduce minor changes to the text and/or graphics, which may alter content. The journal's standard Terms & Conditions and the Ethical guidelines still apply. In no event shall the Royal Society of Chemistry be held responsible for any errors or omissions in this *Accepted Manuscript* or any consequences arising from the use of any information it contains.

ROYAL SOCIETY OF CHEMISTRY

www.rsc.org/pps

Characterizing Rhodopsin Signaling by EPR spectroscopy: From Structure to Dynamics

Ned Van Eps[1], Lydia N. Caro[1], Takefumi Morizumi[1], Oliver P. Ernst[1,2]

[1]Department of Biochemistry, [2]Department of Molecular Genetics,

University of Toronto, Toronto, ON, Canada

E-mail: oliver.ernst@utoronto.ca

Abstract

Electron paramagnetic resonance (EPR) spectroscopy, together with spin labeling techniques, has played a major role in the characterization of rhodopsin, the photoreceptor protein and G protein-coupled receptor (GPCR) in rod cells. Two decades ago, these biophysical tools were the first to identify transmembrane helical movements in rhodopsin upon photo-activation, a critical step in the study of GPCR signaling. EPR methods were employed to identify functional loop dynamics within rhodopsin, to measure light-induced millisecond timescale changes in rhodopsin conformation, to characterize the effects of partial agonists on the apoprotein opsin, and to study lipid interactions with rhodopsin. With the emergence of advanced pulsed EPR techniques, the stage was set to determine the amplitude of structural changes in rhodopsin and the dynamics in the rhodopsin signaling complexes. Work in this area has yielded invaluable information about mechanistic properties of GPCRs. Using EPR techniques, receptors are studied in native-like membrane environments and the effects of lipids on conformational equilibria can be explored. This perspective addresses the impact of EPR methods on rhodopsin and GPCR structural biology, highlighting historical discoveries made with spin labeling techniques, and outlining exciting new directions in the field.

Introduction

Rhodopsin, the photoreceptor protein in rod cells, is a seven transmembrane helix receptor found abundantly in specialized disc membranes in rod cell outer segments. Rhodopsin belongs to the G protein-coupled receptor (GPCR) family and is the eponym of the largest class, the rhodopsin-like GPCRs. Attached via a Schiff base linkage to the apoprotein, opsin, is an 11-*cis* retinal at Lysine 296 (Figure 1). The retinal serves as a covalently attached inverse agonist for rhodopsin, restricting receptor signaling in the absence of light. Upon light absorption by the holoprotein, the chromophore undergoes with high quantum yield (~0.67) ultrafast (~200 fs) *cis*-to-*trans* isomerization that triggers structural and dynamical changes in rhodopsin (reviewed in ref.[1,2]). Allosteric pathways in the receptor link its chromophore pocket to the cytoplasmic binding surface allowing the retinal configuration to regulate receptor dynamics. Reciprocal chromophore–protein interactions increase the quantum yield from 0.23 for retinal in solution[3] to enable the highly efficient and selective photochemistry of rhodopsin. Once rhodopsin is light-activated, it interacts with intracellular signaling partners such as its cognate heterotrimeric G protein transducin, arrestin, and rhodopsin kinase (GRK1). Here we review past and current electron paramagnetic resonance (EPR) spectroscopy studies performed on rhodopsin to characterize conformational dynamics and structural changes in the protein upon photo-activation and signaling. EPR techniques promise to uncover critical aspects of rhodopsin signaling that are important for function and continue to reveal allosteric properties of this prototypical GPCR.

In the late 80's and 90's, Wayne L. Hubbell and colleagues developed EPR methods that biophysically probe conformational changes, solvent accessibility, and backbone dynamics in proteins. These methods dubbed "site-directed spin labeling" (SDSL) combined the molecular biology technique of site-directed mutagenesis with the biophysical tools of EPR spectroscopy.[4,5] The SDSL methodology uses site-specific cysteine mutations on a gene construct depleted of reactive cysteine residues to uniquely introduce labeling sites for nitroxide attachment in proteins (Figure 2). Modern spin labeling applications also use orthogonal labeling schemes for proteins that contain functionally important cysteine side chains.[6,7] Soon after SDSL was introduced, it was applied heavily to study the activation events within recombinantly produced bacteriorhodopsin (bR) and bovine rhodopsin proteins (reviewed in references[8,9]). SDSL has also been used with other retinal proteins such as sensory rhodopsin,[10,11] proteorhodopsin,[12] and channelrhodopsin.[13,14] A summary of the rhodopsin studies is described below with discussions about the different directions of membrane protein EPR in the field.

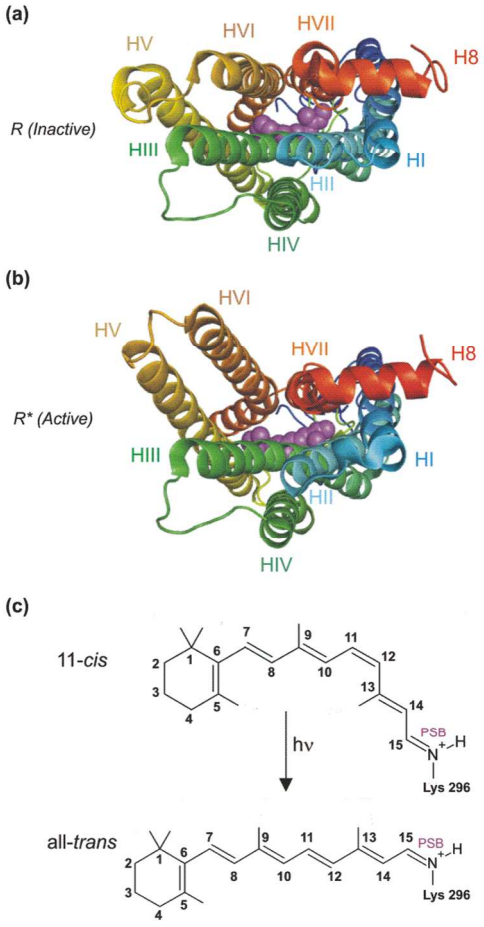

Figure 1. Structure of inactive (R) and active rhodopsin (R*) looking down upon the cytoplasmic surface of the protein. (a) The inactive structure of the receptor (PDB entry: 1GZM). The 11-*cis* retinal is represented by purple spheres, and each helix (labeled HI to HVII for transmembrane helices and H8 for the subsequent cytoplasmic helix) has a distinct color. (b) The active state structure of the receptor (PDB entry: 3PXO). The all-*trans*-retinal is represented by purple spheres, and each helix is colored as in (a). (c) Photo-isomerization of the 11-*cis* retinal occurs within femtoseconds after light absorption forming an all-*trans* isomer with a protonated Schiff base (PSB). Subsequent protein conformational changes include internal Schiff base proton transfer, changes in hydrogen bonding networks involving the Schiff base counterion Glu113 on helix III, and transmembrane helix movements. These events regulate the structural dynamics of rhodopsin. For review see references[1,2].

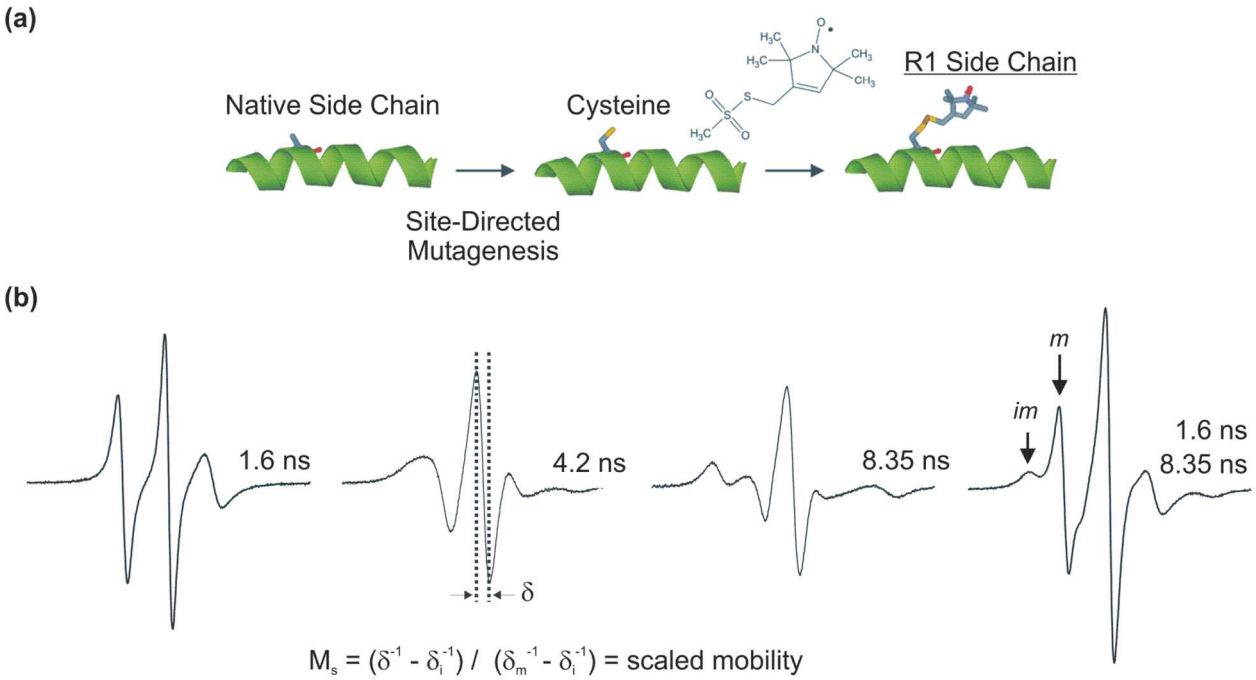

Figure 2. Site-directed spin labeling and interpretation of EPR spectra. (a) Site-directed mutagenesis is used to introduce cysteines for reaction with the functional group of methanethiosulfonate nitroxide spin labels. A paramagnetic nitroxide side chain R1 is generated. (b) Simulated nitroxide spectral lineshapes using the rotational correlation times indicated.[15] The far right spectrum is a composite with two components. The rotational correlation time of each component is shown. The components are labeled immobile (*im*) and mobile (*m*), respectively. Scaled mobility parameters (M_s) can be extracted from experimental spectra by measuring the central linewidth, δ, of R1 at the site of interest. δ_i is the corresponding width for the most immobilized R1, and δ_m is the width for the most mobile R1 in the protein of interest. In addition to the scaled mobility method, EPR spectra can also be fitted to determine nitroxide rotational correlation times (τ) and order parameters (S) using the Microscopic Order / Macroscopic Disorder (MOMD) model.[15]

Conformational changes and loop dynamics in rhodopsin

SDSL can probe local environmental changes around nitroxide spin labels and yields information about backbone dynamics of tethered protein segments,[16,17] as well as site-specific changes in solvent accessibility.[18] Rhodopsin characterization by SDSL was pioneered by the groups of Wayne L. Hubbell and H. Gobind Khorana in the 90's. In a scientific tour de force, nitroxides were placed on a multitude of sites on rhodopsin's cytoplasmic surface that enabled identification of site-specific transmembrane helical movements within the receptor upon light activation.[9] Specifically, movements in

transmembrane helix VI were identified as being crucial for rhodopsin activation.[19,20] These initial studies laid a general framework for current studies on GPCR and other membrane proteins by EPR. Differences between receptor cytoplasmic loop dynamics were also quantitated in these studies by measuring spin label mobility (assessed by a scaled mobility parameter, Figure 2b) throughout the cytoplasmic surface.[9] This work revealed that two receptor cytoplasmic elements are extremely flexible on the protein surface: (i) the C-terminus of the receptor, and (ii) the third cytoplasmic loop (CL-3), which connects helices V and VI in rhodopsin (Figure 3).

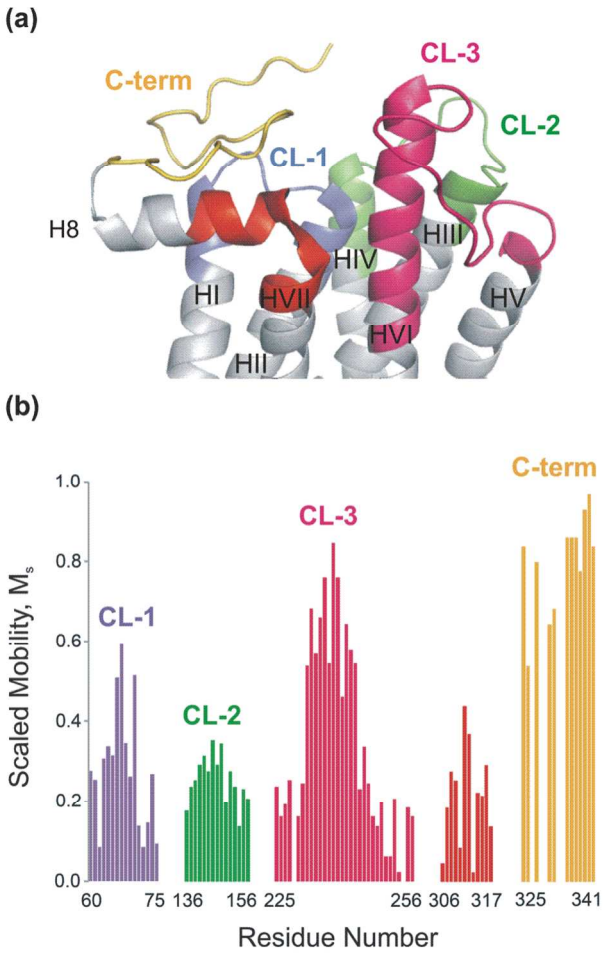

Figure 3. Dynamics of the cytoplasmic surface loops of rhodopsin. (a) Rhodopsin's cytoplasmic loops are color-coded to match the measured scaled mobility parameters shown in (b). Scaled mobility (M_S) parameters of residues in rhodopsin's cytoplasmic surface were taken from ref.[16]. The values of δ_i = 8.4 Gauss and δ_m = 2.1 Gauss were used to calculate M_S.[16] The cytoplasmic loop CL-3, together with the receptor C-terminus, shows the greatest dynamics, consistent with molecular dynamics simulations that identified CL-3 as intrinsically unstructured.[21]

The dynamics of the receptor C-terminus regulates its recognition by binding partners such as arrestin and rhodopsin kinase, while CL-3 is known to be vital for G protein, arrestin, and kinase binding interactions. Importantly, the dynamics observed via biophysical SDSL techniques were confirmed after crystal structures of rhodopsin's dark state became available, (*i.e.* crystal structures showed heterogeneity in CL-3 and have missing electron density in the C-terminus of several structures).[22-24] In the GPCR family, CL-3 shows the most diversity in its length relative to other cytoplasmic surface loops.[25] It is likely that the variability in the loop structure as well as in the positions of transmembrane helices V and VI will lead to signal adaptation in various GPCRs. Coordinated motions between the conserved receptor NPxxY$(X)_{5,6}$F motif (at the helix VII/VIII interface),[26] the C-terminus of rhodopsin, and CL-3 are critical for intracellular signaling (reviewed in references[1,2]).

Time-resolved EPR and the kinetics of rhodopsin conformational change

Time-resolved EPR, in association with other techniques, is used to determine temporal sequences of rhodopsin activation. In continuous wave (CW) EPR, millisecond and longer timescale dynamics can be readily measured using perturbation techniques such as flash-photolysis (FP) EPR. Protein FP-EPR data were first shown for bR[27-30] and the method was later applied to rhodopsin signaling with good time resolution (*i.e.* low millisecond time regime).[31,32]

Time-resolved EPR experiments on bR helped establish the correlation between photocycle intermediates and conformational changes. Absorption measurements at 410 nm (M intermediate) and 570 nm (bR) were compared to EPR spectral changes. This allowed one to determine the nature of the movement of helices F and G as well as cytoplasmic loops of bR and their relation with photocycle reactions.[27-30]

Knierim *et al.* studied the time-resolved movement of helix VI in rhodopsin after illumination.[31] Three approaches were combined: UV-visible spectral measurements (Metarhodopsin II (MII) formation at 380 nm), proton uptake measurements using a pH sensing dye called bromocresol purple (BCP, λ=595 nm), and CW EPR. 227R1 (label R1 at position 227; at the cytoplasmic end of helix V) was used as a reporter of helix VI outward movement because the nitroxide becomes more immobilized following rigid body motion of helix VI. The information obtained from these techniques was used to determine the temporal sequence of late rhodopsin activation events: (i) Internal Schiff base proton transfer, (ii) helix VI motion, and (iii) proton uptake from solution.[31] At low temperatures, the formation of MII becomes rate limiting, and all three processes run parallel with the formation of MII (Figure 4). It was shown that

helix VI motion does not coincide with Schiff base deprotonation at high temperatures (Figure 4b). Proton uptake, however, occurs on a similar time course as helix VI motion, but is a consequence of helix VI outward movement as helix VI motion also takes place at high pH where proton uptake does not occur.[31] It was concluded that MII consists of three isospectral substates, termed MIIa, MIIb and $MIIbH^+$, which are in thermodynamic equilibrium and arise from Metarhodopsin I (MI) according to the following scheme:

$$MI \rightleftharpoons MIIa \rightleftharpoons MIIb \rightleftharpoons MIIbH^+$$

These equilibria of metarhodopsin states are also observed in disc membranes.[33] Furthermore, EPR spectroscopy gave the first indication that motion of helix VI is necessary for binding of a peptide corresponding to the C-terminus of the transducin Gα subunit.[31] This is consistent with the binding of the Gα C-terminus observed in crystal structures of active opsin or MII in complex with C-terminal transducin peptides,[34-36] or β_2-adrenergic receptor in complex with the G protein, $G\alpha_s$.[37]

Furthermore, a time-resolved EPR study with native disc membranes reported the binding of C-terminal transducin peptides to rhodopsin.[32] TOAC and/or proxyl spin labels were covalently attached to transducin C-terminal peptides to study the kinetics of peptide binding and dissociation, and conformational changes in the peptide. EPR spectral changes upon laser photolysis were monitored at the center field trough of the TOAC peptide and followed the formation of the bound species. The time constant for binding to native rhodopsin was ~6 ms at 295 K. The rate of formation of the active state of rhodopsin, which is slower in membranes than in dodecyl maltoside (DDM) micelles, appeared to limit the rate of peptide binding.

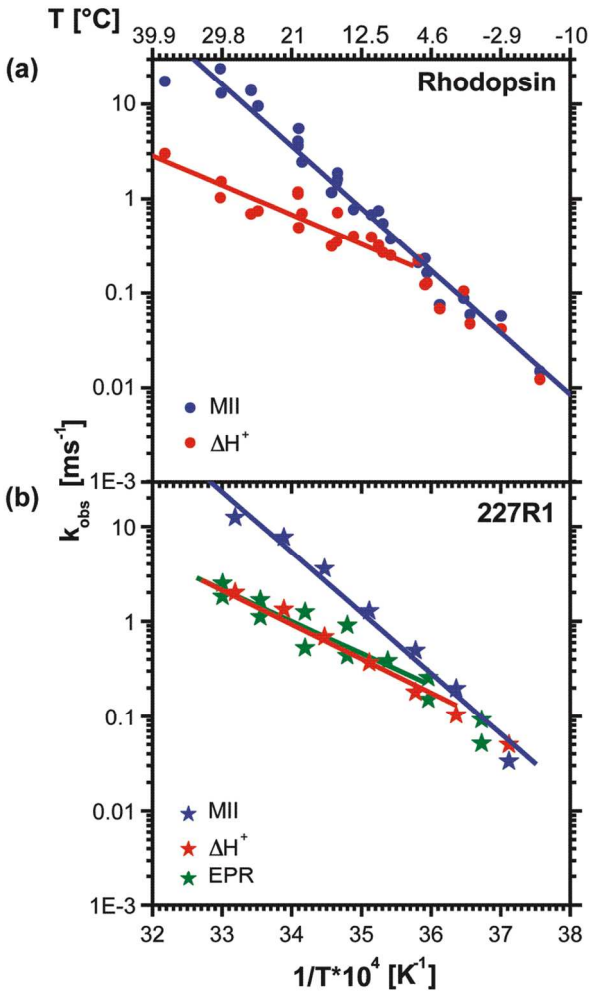

Figure 4. Arrhenius plots of the rate constants for MII formation, proton uptake, and helix VI motion. Data were taken from reference [31]. (a) Wild-type rhodopsin in DDM. Rates of MII formation (blue dots) and proton uptake (red dots). (b) Data for rhodopsin 227R1 in DDM, including rate data from EPR measurements that reflect helix VI movement (green stars).

Double Electron–Electron Resonance (DEER) spectroscopy characterization of rhodopsin signaling

Pulsed dipolar spectroscopy techniques (*i.e.* DEER, Double Quantum Coherence, etc.) are advanced biophysical tools used to measure distance distributions between pairs of stable radicals. The four pulse DEER method was developed by Spiess and colleagues in 2000,[38] and was first used in the GPCR community in 2006 by coupling it to SDSL methodology.[39] C-terminal helix movements in a G protein α-subunit were shown to be a trigger for GDP release upon rhodopsin binding (Figure 5).[39] Two nitroxide labels were placed in the Gα subunit of the G protein heterotrimer and used to sense the protein motion. One site was located in the conformationally dynamic C-terminus (α5 helix) and the other was a reference site in a neighboring β-sheet. Upon receptor binding, the inter-spin distance (*i.e.*, NO•–NO•) between the labels changed and reflected α5 helix movement away from the reference site. This was direct evidence showing that C-terminal perturbations are linked to GDP release in the G protein.[39]

A crystal structure of active opsin in complex with a C-terminal transducin peptide identified a binding site of the α5 helix on the active receptor and supported, together with docking studies, the conclusion obtained from the EPR data.[34,40] The perturbation of the α5 helix might be a general feature of G protein signaling as this was later also observed in the crystal structure of the β_2-adrenergic receptor in complex with the G protein, $G\alpha_s$, where the α5 helix was rotated and displaced relative to the body of the Ras-like domain toward the receptor (Figure 5c).[37]

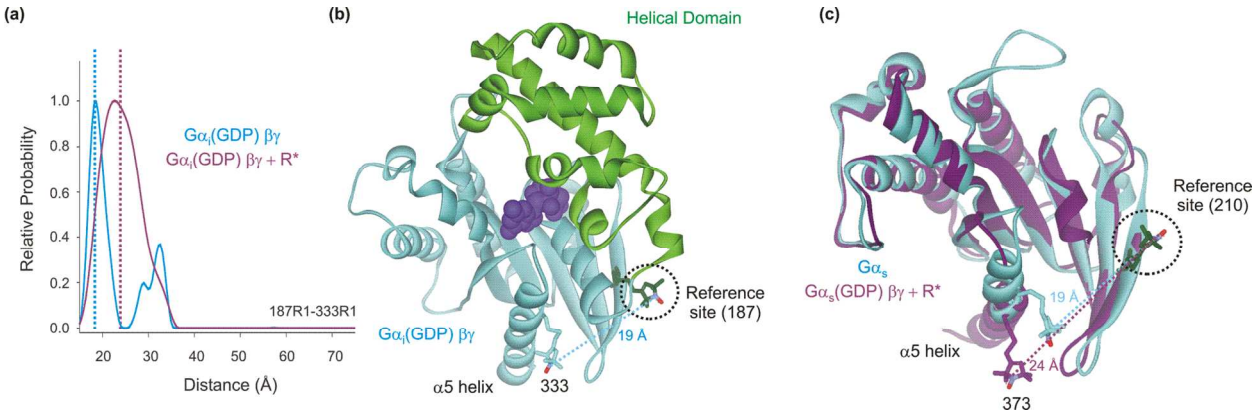

Figure 5. Inter-spin distance changes in $G\alpha_i$ subunits upon interaction of G protein and light-activated rhodopsin, R*.[39] (a) The distance between nitroxide labels at positions 187 and 333 of $G\alpha_i$ increases in the presence of R* and a broader distribution of distances centered at 24 Å is observed in the R*-bound state. (b) Molecular modeling of the R1 side chain at positions 187 and 333 of $G\alpha_i$ suggests an inter-nitroxide distance of approximately 19 Å. (c) Structural overlay of the $G\alpha_s$ Ras-like domain in receptor-bound (purple, residues 40 to 394) and unbound (cyan, residues 41 to 379) conformational states (PDB entries 3SN6 and 1AZT). Binding of the β_2-adrenergic receptor forces separation between the α5 helix and a reference site in the β2 sheet of $G\alpha_s$ (green sticks).[37] By modeling nitroxide labels into the corresponding positions as in $G\alpha_i$,[39] an analogous 5 Å displacement of the α5 helix in $G\alpha_s$ upon GPCR binding is observed.

DEER, together with SDSL, has become an informative way of probing functional conformational changes in GPCR signaling systems. An example is an extensive study showing how the cytoplasmic surface of rhodopsin is changed upon light activation.[41] In this study, Altenbach and coworkers pairwise

spin-labeled all seven transmembrane helices, as well as helix VIII on the cytoplasmic surface of rhodopsin, and measured distances between the spin label pairs. Upon light activation, the receptor in DDM micelles showed a 5 Å outward movement of helix VI as well as other small helical movements. These results suggest that SDSL-DEER can be applied to any GPCR that can be expressed recombinantly.

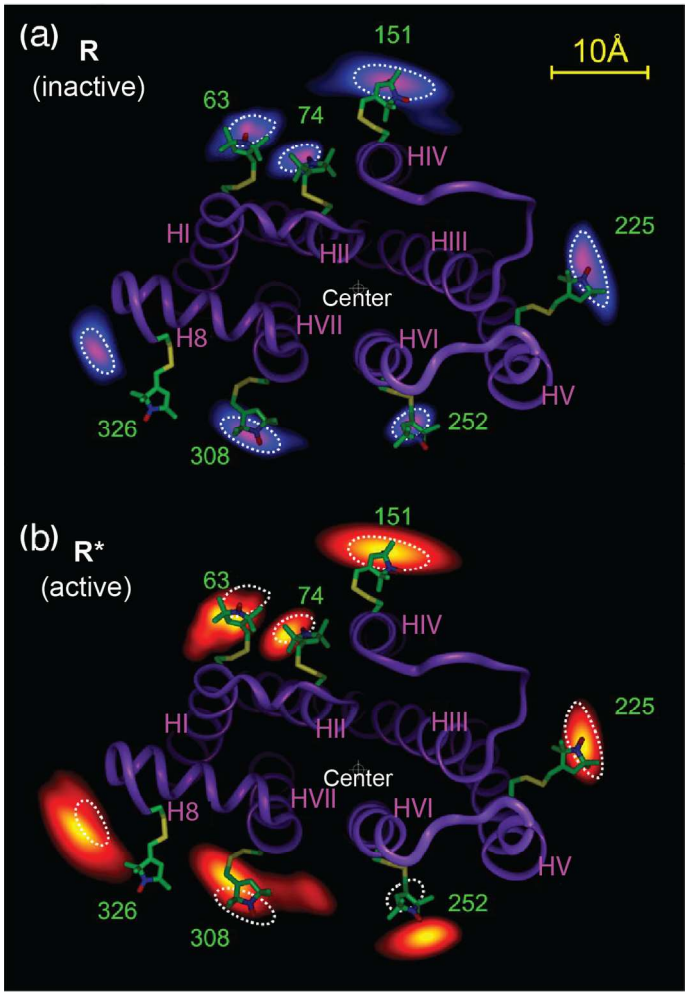

Figure 6. Projection contours of the spin locations calculated from the measured distance distributions for representative nitroxide sites.[41] (a) Probable locations of the nitroxide spins in **R** shown in a gradient from blue to purple and overlaid on a ribbon model of **R** from the dark state rhodopsin crystal structure (PDB entry 1GZM). (b) Corresponding locations in light-activated rhodopsin, **R***, shown in a gradient from red to yellow, and, for reference, the ribbon model and typical contours (dotted traces) for **R** overlaid. The figure was modified from reference [41].

Partial agonism of GPCRs

In addition to native ligands, synthetic ligands can activate or inhibit GPCRs as pharmaceuticals. The ligands are classified as full or partial agonists, full or partial inverse agonists, or antagonists, respectively, depending on whether the receptor activity in the presence of the ligand, and thus the cellular response, is increased, decreased or unaffected relative to the basal activity of the ligand-free GPCR. In recent years, some ligands dubbed "biased agonists" have been found to modulate G protein-independent cellular signaling pathways that originate from arrestin (reviewed in ref.[42]). The small molecule ligands modulate GPCR function by altering the conformational equilibrium of the receptor. While crystallographic studies have provided a number of ligand bound GPCR structures and new insights (reviewed in references[43,44]), molecular details of GPCR function are not yet completely understood. Helix movements appear to be similar in GPCRs, but the extent of helix motion and conformational equilibria may vary between receptors. Crystallographic snapshots of low-energy receptor conformations may not be ideal for comparing GPCR conformations due to frequent use of thermostabilization and/or fusion partners for GPCR crystallization. So far, rhodopsin is the only GPCR whose fully active and inactive structures have been crystallized using entirely native sequences,[22-24,35,45] thus avoiding protein engineering that can influence and mask structural changes. However, crystallization conditions can have an effect on receptor conformation. For example, octyl glucoside detergent can stabilize the active opsin conformation and promote crystallization of a specific receptor conformation.[46] Therefore, understanding the function of rhodopsin, and of GPCRs in general, needs additional biophysical tools like fluorescence, infrared, EPR and NMR spectroscopy to address protein dynamics.[47]

As described above, light-activated rhodopsin exists in an equilibrium of states and different retinal ligands can potentially affect this equilibrium and populate somewhat different conformations. This is an area where EPR spectroscopy can provide insight. For rhodopsin, a number of modified chromophore ligands have been reported to have effects on formation of the light-induced intermediate states, as observed by UV-visible and Fourier transform infrared (FTIR) spectroscopy.[48-54] Although these studies were originally aimed at observing local environmental changes between ligands and the protein moiety, the effect on active state formation is likely the same as observed for partial agonists on other GPCRs.

To further investigate the spectroscopic findings described above, the conformational differences between rhodopsin bound to the full agonist (all-*trans*-retinal) and a partial agonist (all-*trans* 9-

demethyl-retinal)[54,55] were studied using SDSL and EPR spectroscopy.[56] 9-demethyl retinal (9-dm-retinal) is lacking the methyl group at carbon atom C9 (Figure 1). In contrast to crystallography, SDSL-EPR cannot provide structural information on the entire protein, but can detect local structural changes with high sensitivity. Moreover, a great advantage is that the measurements can be performed in solution and in membranes. Thus, unnatural contacts between proteins can be avoided, such as those observed in a crystal lattice. In DDM solution, a spin label at position 227 (cytoplasmic end of helix V) of rhodopsin clearly sensed the reduced population of displaced helix VI by all-*trans* 9-dm-retinal relative to all-*trans*-retinal (Figure 7a). A shift of the MI/MII equilibrium was also observed by FTIR for light-activated pigments reconstituted initially with 9-*cis* 9-dm-retinal.[53] Furthermore, the activating mutation E134Q, which anticipates proton uptake in MIIb, increased the population of all-*trans* 9-dm-retinal containing metarhodopsins with displaced helix VI (Figure 7b). These results are consistent with previous findings regarding the reduction and restoration of G protein activity observed for different 9-dm-pigments (Figure 7c).[55]

Similarly to rhodopsin studies with 9-dm-retinal analogs, partial agonism of GPCRs could be explained by the fractional population changes of two helix VI positions and different interconversion rates. These changes could also be detected using DEER spectroscopy on receptors with pairs of spin label sensors. By using a set of doubly spin-labeled rhodopsin pigments or GPCRs, EPR/DEER spectroscopy can provide a precise mapping of local structural changes to identify changes in the equilibrium of GPCR states. This approach will be very valuable to investigate the mode of action of biased agonists to understand selection between G protein-dependent and G protein-independent signaling pathways.

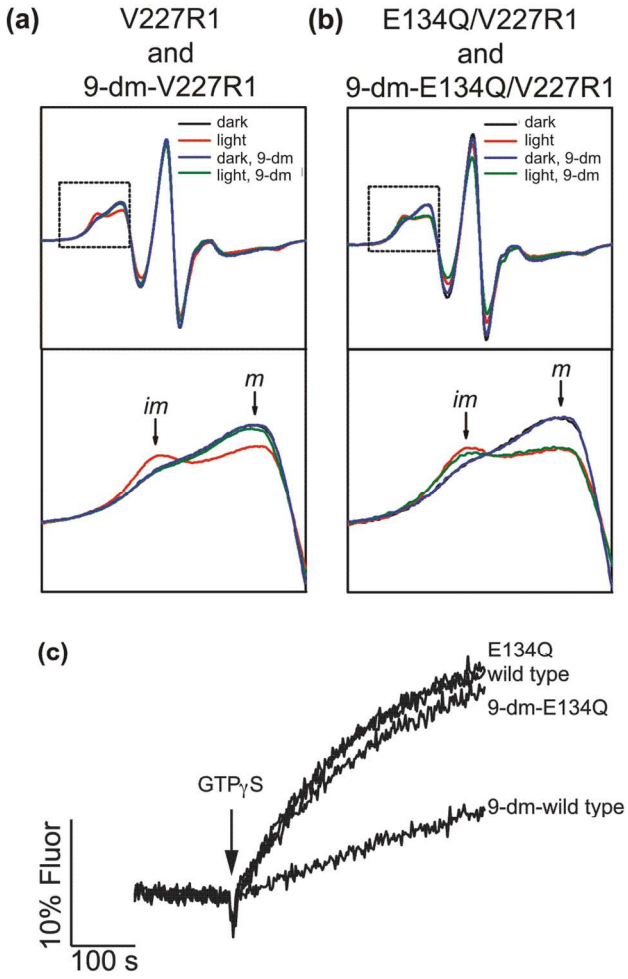

Figure 7. Partial agonism observed in DDM-solubilized rhodopsin pigments reconstituted with 9-dm-retinal. Figures were adapted from references [55,56]. (a) EPR spectra of the V227R1 rhodopsin mutant reconstituted with retinal or 9-dm-retinal, yielding 9-dm-pigments. Spectra were recorded at 25 °C and pH 7.5 in the dark and after illumination with orange light for 15 s. For clarity, the low field regions are expanded in the lower *panel* and components corresponding to immobile (*im*) and mobile (*m*) nitroxides are indicated by arrows. All spectra are normalized to the height of the central resonance line in order to compare the line shapes. (b) EPR spectra of the E134Q/V227R1 mutant reconstituted with 9-dm-retinal. (c) Transducin activation by wild type, 9-dm-wild type, E134Q, and 9-dm-E134Q pigments. The reaction was initiated by addition of GTPγS. The *scale bars* indicate a 10% fluorescence increase and 100 s, respectively.

Membranes, rhodopsin and EPR

Rhodopsin resides in specialized disc membranes found in rod outer segments. These membranes are comprised of ~45 mol% phosphatidylcholine (PC), ~41 mol% phosphatidylethanolamine (PE), ~13 mol% phosphatidylserine (PS) and ~2 mol% phosphatidylinositol (PI).[57] Compared with plasma membranes, disc membranes are very rich in PE, and docosahexaenoic acid (DHA) acyl chains are frequently found in disc membrane lipids (35% vs. 5% (w/w) of the total fatty acids in disc and plasma membranes, respectively).[58] Lipids containing polyunsaturated DHA chains contribute to high membrane fluidity. The cholesterol content of discs ranges from 5–30 mol% along the rod outer segment (apical to basal membranes) and affects stability and activity of rhodopsin (reviewed in ref.[59]). It appears that the disc membrane lipid composition is optimized for visual signaling as the function of rhodopsin depends on the lipid matrix (reviewed in ref.[60]).

A critical factor for rhodopsin function is the MI/MII equilibrium, which is very sensitive to the lipid composition. Curvature elastic stress, membrane fluidity and direct interaction with annular lipids (surrounding rhodopsin) are reported to be responsible for shifting the MI/MII equilibrium (Figure 8).[61] Cholesterol was shown to strongly inhibit rhodopsin by favoring the formation of the non-signaling intermediate MI.[62,63] Two different modes of action can explain this effect: (i) cholesterol reduces the phospholipid acyl chain packing free volume in the bilayer and increases lipid ordering[63,64] (Figure 8b), and (ii) cholesterol interacts specifically with rhodopsin as shown by FRET studies[65] and as suggested by MD simulations[66] (Figure 8c). Sequence alignment studies have detected putative cholesterol recognition amino acid consensus sequences in helices I, III and VII of rhodopsin.[67] A specific binding site for cholesterol was found in a crystal structure of the β_2-adrenergic receptor.[68] Cholesterol is also known to modulate function and interactions of other GPCRs.[69]

Besides cholesterol, several membrane components have been reported to shift the MI/MII equilibrium. The shift towards MI or MII is thereby dependent on the type of lipid headgroup as well as length and number of double bonds of the fatty acid chain. The origins of these effects reside in curvature forces in lipid–protein interactions and hydrophobic mismatch, which corresponds to a mismatch between the lipid bilayer thickness and the hydrophobic surface of the receptor that arises from light-induced conformational changes in rhodopsin (Figure 8a, for details see references[60,70]). In addition, specific lipid–rhodopsin interactions were found by FTIR spectroscopy.[71]

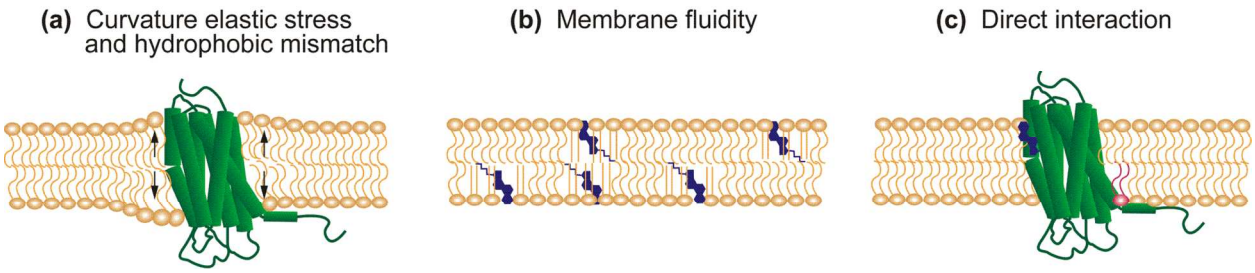

Figure 8: Ways lipids affect metarhodopsin conformations. (a) Lipids under curvature elastic stress and hydrophobic mismatch influence the MI/MII equilibrium. (b) Cholesterol (in dark blue) alters membrane fluidity and lateral lipid packing density. (c) Lipids (*e.g.*, phospholipid depicted in red or cholesterol depicted in blue) can directly interact with rhodopsin and shift the MI/MII equilibrium.

Use of nanodiscs for EPR studies. For best characterization of rhodopsin by EPR, studies are ideally done in reconstituted membrane-mimicking environments with carefully controlled lipid composition. In the past, most studies were performed in DDM solution, but reconstitution of rhodopsin in nanodiscs[72] is becoming more popular as the receptor can be studied under more native conditions. Nanodiscs are lipid discs encircled by two amphipathic membrane scaffold proteins (MSP) derived from the human apolipoprotein A1. Nanodiscs have been frequently used for rhodopsin studies.[73-78] Due to their symmetry, nanodiscs have the advantage of not displaying preferred orientation for transmembrane protein insertion. Overall, nanodiscs can be considered as good membrane mimics, although EPR studies with paramagnetic PC lipids showed that the surrounding MSP affects lipid fluidity.[79] The ability to control the lipid composition to improve rhodopsin coupling to binding partners (transducin, arrestin, GRK1) allows the use of DEER spectroscopy to map distances within these complexes. This can give rise to models of GPCR complexes where data are very challenging to obtain using protein crystallography. DEER spectroscopy (as described above) can be used to support crystal structures of a complex, rule out crystal artifacts, as well as determine conformational substates and heterogeneity within the complexes.

Information obtained from EPR studies on rhodopsin in membrane-like environments. Much current work on rhodopsin in lipid environments has been focused on investigating UV-visible spectral shifts (*i.e.* Schiff base protonation state changes) and FTIR difference spectra and has not probed sequence-specific conformational changes in the receptor distant from the retinal pocket. To date, only a few EPR studies

on rhodopsin structure and dynamics have been conducted in a synthetic membrane environment. The dynamics of the cytoplasmic surface of rhodopsin upon light activation in micelles and liposomes has been previously investigated.[80] Residues 140, 227, 250 and 316 were selected and mutated individually to cysteine residues for SDSL.[80] In order to assess the mobility of the nitroxide label at these positions, CW EPR spectroscopy was performed in DDM, digitonin micelles, and liposomes (POPC:POPE:POPS, 5:4:1 molar ratio), at different pH values and temperatures. The following differences in nitroxide side chain motion were observed when comparing liposomes and DDM: (i) 140R1 (helix III) was more immobilized in liposomes relative to DDM micelles, but both environments showed no light-induced conformational changes at 20 °C; (ii) light-induced conformational changes were retained in lipids in the case of 227R1 (helix V), but the amplitude of the change was reduced, (iii) 250R1 (helix VI), which is not in contact with the lipid bilayer, showed a similar spectrum as in DDM, although the mobile component was less populated in liposomes, (iv) when a spin label was introduced at position 316, both mobile and immobile components were present, but in different proportions.

For the residues that are situated in close contact with the membrane, the difference between detergent and membrane can be explained by steric constraints caused by lipids (*i.e.*, in the case of 140R1) or the existence of metarhodopsin states that are not observed in DDM (namely, MI). In the case of 316R1, which is located in helix VIII, the discrepancy in the CW spectra observed between the lipid environment and detergent could be explained by a change in local environment in the label vicinity.

Experiments on the pH dependence of the receptor were done using site 250R1 to study rhodopsin equilibria after light activation. Using different pH values, it was reported that both MIIa and MIIb coexist in DDM and liposomes. Figure 9 shows EPR data collected in DDM micelles compared to liposomes at pH 6.0 and 20°C. Differences in the amount of the immobilized species are observed between the environments.

When CW EPR spectra were measured on rhodopsin solubilized in digitonin micelles, the conformational changes were hindered to the point that an increase in A_{380} (*i.e.* Schiff base deprotonation) was not correlated with the helix VI movement anymore.[80] This shows that the solubilizing environment in which a membrane protein is characterized should be carefully selected and that UV-visible measurements of rhodopsin do not always directly reflect structural changes on rhodopsin's cytoplasmic surface.

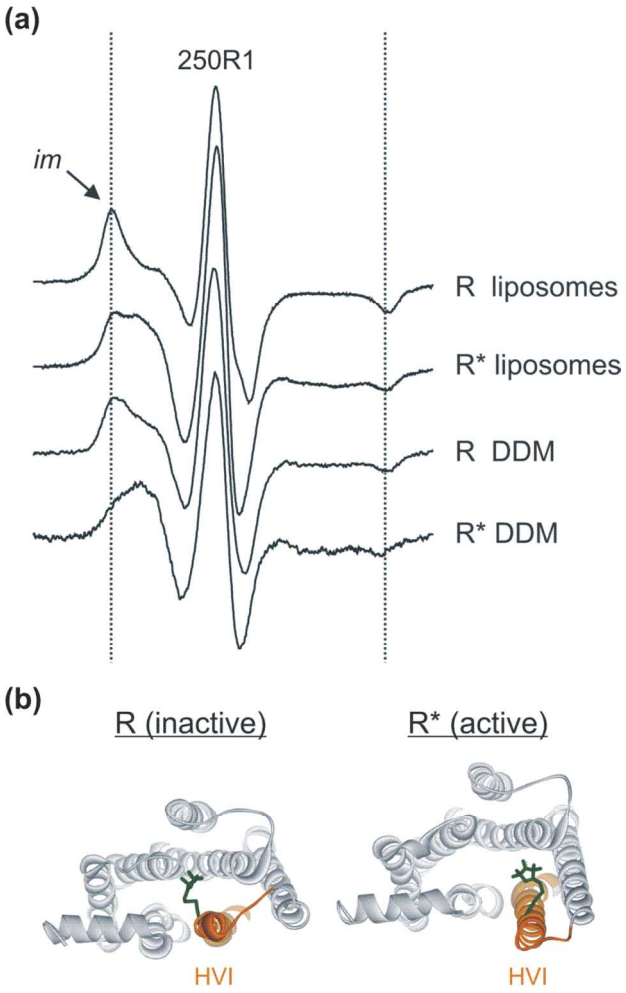

Figure 9. Experimental EPR spectra of rhodopsin 250R1 in DDM and POPC:POPE:POPS bilayers at pH 6.0 and 20 °C.[80] Position 250 is at the cytoplasmic end of helix VI (HVI) and spin label R1 can sense the closed (inactive; R and MI) and open (active; MII) receptor conformations (*bottom*). Immobile (*im*) components in the spectra are indicated by the arrow. In liposomes, more of the immobilized species is seen in the R and R* spectra relative to DDM due to lateral membrane pressure favoring the closed conformation.

Finally, spin-labeled lipids combined with CW EPR can identify lipids that are restricted in their motions by contacts with a membrane protein (annular lipids). In a CW EPR spectrum, bulk lipids appear as a mobile component in CW EPR spectra while annular lipids are represented by a strongly immobilized component. In the late 70's, early 80's, such studies were done in rod outer segment membranes.[81,82]

This technique was applied to various membrane proteins to calculate the association constant for paramagnetic lipids (reviewed in ref.[83]).

Conclusions and Outlook

Advanced EPR methodologies are critical for the characterization of rhodopsin signaling and for understanding the role of protein dynamics in photo-transduction. The use of these techniques in the coming years will unveil vital information about rhodopsin and other GPCRs. Monitoring structural dynamics of rhodopsin at its cytoplasmic surface will yield insight into binding partner selectivity (*e.g.* G proteins, kinases and arrestins). It is unlikely that rhodopsin's active state will be structurally identical with each different binding partner. In addition, understanding the allosteric pathways between the ligand binding pocket and the cytoplasmic surface is crucial for a comprehensive understanding of photo-signaling. Mutations that disrupt allosteric networks can lead to altered receptor phenotypes and GPCR disease states. Finally, exploring ligand channels within rhodopsin and other GPCRs will be possible with small molecule compounds and strategically placed EPR sensor labels.

Acknowledgements

We thank Aidin R. Balo, WeiLin Ou, Emil Pai and Scott Prosser for comments on the manuscript. This work was supported by the Canada Excellence Research Chair program. O.P.E. holds the Anne and Max Tanenbaum Chair in Neuroscience at the University of Toronto.

Graphical Abstract

Perspective on how EPR spectroscopy brings insights into rhodopsin and GPCR dynamics

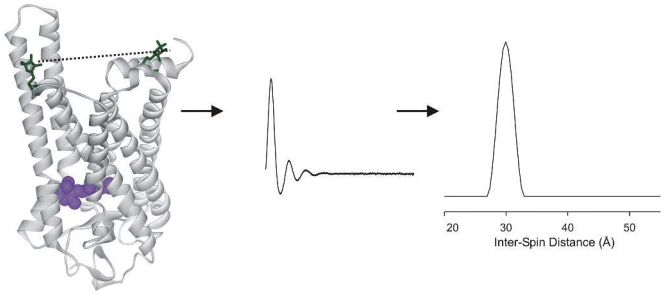

References

1. O. P. Ernst, D. T. Lodowski, M. Elstner, P. Hegemann, L. S. Brown and H. Kandori, Microbial and animal rhodopsins: structures, functions, and molecular mechanisms, *Chem. Rev.*, 2014, **114**, 126-163.
2. K. P. Hofmann, P. Scheerer, P. W. Hildebrand, H. W. Choe, J. H. Park, M. Heck and O. P. Ernst, A G protein-coupled receptor at work: the rhodopsin model, *Trends Biochem. Sci.*, 2009, **34**, 540-552.
3. Y. Koyama, K. Kubo, M. Komori, H. Yasuda and Y. Mukai, Effect of protonation on the isomerization properties of n-butylamine Schiff base of isomeric retinal as revealed by direct HPLC analyses: selection of isomerization pathways by retinal proteins, *Photochem. Photobiol.*, 1991, **54**, 433-443.
4. C. Altenbach, T. Marti, H. G. Khorana and W. L. Hubbell, Transmembrane protein structure: spin labeling of bacteriorhodopsin mutants, *Science*, 1990, **248**, 1088-1092.
5. C. Altenbach, S. L. Flitsch, H. G. Khorana and W. L. Hubbell, Structural studies on transmembrane proteins. 2. Spin labeling of bacteriorhodopsin mutants at unique cysteines, *Biochemistry*, 1989, **28**, 7806-7812.
6. M. R. Fleissner, E. M. Brustad, T. Kalai, C. Altenbach, D. Cascio, F. B. Peters, K. Hideg, S. Peuker, P. G. Schultz and W. L. Hubbell, Site-directed spin labeling of a genetically encoded unnatural amino acid, *Proc. Natl. Acad. Sci. U. S. A.*, 2009, **106**, 21637-21642.
7. M. J. Schmidt, J. Borbas, M. Drescher and D. Summerer, A genetically encoded spin label for electron paramagnetic resonance distance measurements, *J. Am. Chem. Soc.*, 2014, **136**, 1238-1241.
8. J. P. Klare, Site-directed spin labeling EPR spectroscopy in protein research, *Biol. Chem.*, 2013, **394**, 1281-1300.
9. W. L. Hubbell, C. Altenbach, C. M. Hubbell and H. G. Khorana, Rhodopsin structure, dynamics, and activation: a perspective from crystallography, site-directed spin labeling, sulfhydryl reactivity, and disulfide cross-linking, *Adv. Protein Chem.*, 2003, **63**, 243-290.
10. J. Sasaki, B. J. Phillips, X. Chen, N. Van Eps, A. L. Tsai, W. L. Hubbell and J. L. Spudich, Different dark conformations function in color-sensitive photosignaling by the sensory rhodopsin I-HtrI complex, *Biophys. J.*, 2007, **92**, 4045-4053.

11. E. Bordignon, J. P. Klare, J. Holterhues, S. Martell, A. Krasnaberski, M. Engelhard and H. J. Steinhoff, Analysis of light-induced conformational changes of Natronomonas pharaonis sensory rhodopsin II by time resolved electron paramagnetic resonance spectroscopy, *Photochem. Photobiol.*, 2007, **83**, 263-272.
12. D. T. Edwards, T. Huber, S. Hussain, K. M. Stone, M. Kinnebrew, I. Kaminker, E. Matalon, M. S. Sherwin, D. Goldfarb and S. Han, Determining the oligomeric structure of proteorhodopsin by Gd3+ -based pulsed dipolar spectroscopy of multiple distances, *Structure*, 2014, **22**, 1677-1686.
13. T. Sattig, C. Rickert, E. Bamberg, H. J. Steinhoff and C. Bamann, Light-induced movement of the transmembrane helix B in channelrhodopsin-2, *Angew. Chem. Int. Ed. Engl.*, 2013, **52**, 9705-9708.
14. N. Krause, C. Engelhard, J. Heberle, R. Schlesinger and R. Bittl, Structural differences between the closed and open states of channelrhodopsin-2 as observed by EPR spectroscopy, *FEBS Lett.*, 2013, **587**, 3309-3313.
15. D. E. Budil, S. Lee, S. Saxena and J. H. Freed, Nonlinear-Least-Squares Analysis of Slow-Motion EPR Spectra in One and Two Dimensions Using a Modified Levenberg–Marquardt Algorithm, *J. Magn. Res.*, 1996, **120**, 155-189.
16. L. Columbus and W. L. Hubbell, A new spin on protein dynamics, *Trends Biochem. Sci.*, 2002, **27**, 288-295.
17. C. J. Lopez, S. Oga and W. L. Hubbell, Mapping molecular flexibility of proteins with site-directed spin labeling: a case study of myoglobin, *Biochemistry*, 2012, **51**, 6568-6583.
18. C. Altenbach, W. Froncisz, R. Hemker, H. McHaourab and W. L. Hubbell, Accessibility of nitroxide side chains: absolute Heisenberg exchange rates from power saturation EPR, *Biophys. J.*, 2005, **89**, 2103-2112.
19. D. L. Farrens, C. Altenbach, K. Yang, W. L. Hubbell and H. G. Khorana, Requirement of rigid-body motion of transmembrane helices for light activation of rhodopsin, *Science*, 1996, **274**, 768-770.
20. C. Altenbach, K. Yang, D. L. Farrens, Z. T. Farahbakhsh, H. G. Khorana and W. L. Hubbell, Structural features and light-dependent changes in the cytoplasmic interhelical E-F loop region of rhodopsin: a site-directed spin-labeling study, *Biochemistry*, 1996, **35**, 12470-12478.
21. M. Elgeti, A. S. Rose, F. J. Bartl, P. W. Hildebrand, K. P. Hofmann and M. Heck, Precision vs flexibility in GPCR signaling, *J. Am. Chem. Soc.*, 2013, **135**, 12305-12312.
22. K. Palczewski, T. Kumasaka, T. Hori, C. A. Behnke, H. Motoshima, B. A. Fox, I. Le Trong, D. C. Teller, T. Okada, R. E. Stenkamp, M. Yamamoto and M. Miyano, Crystal structure of rhodopsin: A G protein-coupled receptor, *Science*, 2000, **289**, 739-745.
23. T. Okada, M. Sugihara, A. N. Bondar, M. Elstner, P. Entel and V. Buss, The retinal conformation and its environment in rhodopsin in light of a new 2.2 A crystal structure, *J. Mol. Biol.*, 2004, **342**, 571-583.
24. J. Li, P. C. Edwards, M. Burghammer, C. Villa and G. F. Schertler, Structure of bovine rhodopsin in a trigonal crystal form, *J. Mol. Biol.*, 2004, **343**, 1409-1438.
25. T. Mirzadegan, G. Benko, S. Filipek and K. Palczewski, Sequence analyses of G-protein-coupled receptors: similarities to rhodopsin, *Biochemistry*, 2003, **42**, 2759-2767.
26. O. Fritze, S. Filipek, V. Kuksa, K. Palczewski, K. P. Hofmann and O. P. Ernst, Role of the conserved NPxxY(x)5,6F motif in the rhodopsin ground state and during activation, *Proc. Natl. Acad. Sci. U. S. A.*, 2003, **100**, 2290-2295.
27. N. Radzwill, K. Gerwert and H. J. Steinhoff, Time-resolved detection of transient movement of helices F and G in doubly spin-labeled bacteriorhodopsin, *Biophys. J.*, 2001, **80**, 2856-2866.
28. T. Rink, J. Riesle, D. Oesterhelt, K. Gerwert and H. J. Steinhoff, Spin-labeling studies of the conformational changes in the vicinity of D36, D38, T46, and E161 of bacteriorhodopsin during the photocycle, *Biophys. J.*, 1997, **73**, 983-993.

29. H. J. Steinhoff, R. Mollaaghababa, C. Altenbach, K. Hideg, M. Krebs, H. G. Khorana and W. L. Hubbell, Time-resolved detection of structural changes during the photocycle of spin-labeled bacteriorhodopsin, *Science*, 1994, **266**, 105-107.
30. T. E. Thorgeirsson, W. Xiao, L. S. Brown, R. Needleman, J. K. Lanyi and Y. K. Shin, Transient channel-opening in bacteriorhodopsin: an EPR study, *J. Mol. Biol.*, 1997, **273**, 951-957.
31. B. Knierim, K. P. Hofmann, O. P. Ernst and W. L. Hubbell, Sequence of late molecular events in the activation of rhodopsin, *Proc. Natl. Acad. Sci. U. S. A.*, 2007, **104**, 20290-20295.
32. N. Van Eps, L. L. Anderson, O. G. Kisselev, T. J. Baranski, W. L. Hubbell and G. R. Marshall, Electron paramagnetic resonance studies of functionally active, nitroxide spin-labeled peptide analogues of the C-terminus of a G-protein alpha subunit, *Biochemistry*, 2010, **49**, 6877-6886.
33. M. Mahalingam, K. Martinez-Mayorga, M. F. Brown and R. Vogel, Two protonation switches control rhodopsin activation in membranes, *Proc. Natl. Acad. Sci. U. S. A.*, 2008, **105**, 17795-17800.
34. P. Scheerer, J. H. Park, P. W. Hildebrand, Y. J. Kim, N. Krauss, H. W. Choe, K. P. Hofmann and O. P. Ernst, Crystal structure of opsin in its G-protein-interacting conformation, *Nature*, 2008, **455**, 497-502.
35. H. W. Choe, Y. J. Kim, J. H. Park, T. Morizumi, E. F. Pai, N. Krauss, K. P. Hofmann, P. Scheerer and O. P. Ernst, Crystal structure of metarhodopsin II, *Nature*, 2011, **471**, 651-655.
36. X. Deupi, P. Edwards, A. Singhal, B. Nickle, D. Oprian, G. Schertler and J. Standfuss, Stabilized G protein binding site in the structure of constitutively active metarhodopsin-II, *Proc. Natl. Acad. Sci. U. S. A.*, 2012, **109**, 119-124.
37. S. G. Rasmussen, B. T. DeVree, Y. Zou, A. C. Kruse, K. Y. Chung, T. S. Kobilka, F. S. Thian, P. S. Chae, E. Pardon, D. Calinski, J. M. Mathiesen, S. T. Shah, J. A. Lyons, M. Caffrey, S. H. Gellman, J. Steyaert, G. Skiniotis, W. I. Weis, R. K. Sunahara and B. K. Kobilka, Crystal structure of the beta2 adrenergic receptor-Gs protein complex, *Nature*, 2011, **477**, 549-555.
38. M. Pannier, S. Veit, A. Godt, G. Jeschke and H. W. Spiess, Dead-time free measurement of dipole-dipole interactions between electron spins, *J. Magn. Reson.*, 2000, **142**, 331-340.
39. W. M. Oldham, N. Van Eps, A. M. Preininger, W. L. Hubbell and H. E. Hamm, Mechanism of the receptor-catalyzed activation of heterotrimeric G proteins, *Nat. Struct. Mol. Biol.*, 2006, **13**, 772-777.
40. P. Scheerer, M. Heck, A. Goede, J. H. Park, H. W. Choe, O. P. Ernst, K. P. Hofmann and P. W. Hildebrand, Structural and kinetic modeling of an activating helix switch in the rhodopsin-transducin interface, *Proc. Natl. Acad. Sci. U. S. A.*, 2009, **106**, 10660-10665.
41. C. Altenbach, A. K. Kusnetzow, O. P. Ernst, K. P. Hofmann and W. L. Hubbell, High-resolution distance mapping in rhodopsin reveals the pattern of helix movement due to activation, *Proc. Natl. Acad. Sci. U. S. A.*, 2008, **105**, 7439-7444.
42. J. W. Wisler, K. Xiao, A. R. Thomsen and R. J. Lefkowitz, Recent developments in biased agonism, *Curr. Opin. Cell Biol.*, 2014, **27**, 18-24.
43. M. Audet and M. Bouvier, Restructuring G-protein- coupled receptor activation, *Cell*, 2012, **151**, 14-23.
44. V. Katritch, V. Cherezov and R. C. Stevens, Structure-function of the G protein-coupled receptor superfamily, *Annu. Rev. Pharmacol. Toxicol.*, 2013, **53**, 531-556.
45. J. H. Park, P. Scheerer, K. P. Hofmann, H. W. Choe and O. P. Ernst, Crystal structure of the ligand-free G-protein-coupled receptor opsin, *Nature*, 2008, **454**, 183-187.
46. J. H. Park, T. Morizumi, Y. Li, J. E. Hong, E. F. Pai, K. P. Hofmann, H. W. Choe and O. P. Ernst, Opsin, a structural model for olfactory receptors?, *Angew. Chem. Int. Ed. Engl.*, 2013, **52**, 11021-11024.

47. A. Manglik and B. Kobilka, The role of protein dynamics in GPCR function: insights from the beta2AR and rhodopsin, *Curr. Opin. Cell Biol.*, 2014, **27**, 136-143.
48. U. M. Ganter, E. D. Schmid, D. Perez-Sala, R. R. Rando and F. Siebert, Removal of the 9-methyl group of retinal inhibits signal transduction in the visual process. A Fourier transform infrared and biochemical investigation, *Biochemistry*, 1989, **28**, 5954-5962.
49. T. Okada, H. Kandori, Y. Shichida, T. Yoshizawa, M. Denny, B. W. Zhang, A. E. Asato and R. S. Liu, Spectroscopic study of the batho-to-lumi transition during the photobleaching of rhodopsin using ring-modified retinal analogues, *Biochemistry*, 1991, **30**, 4796-4802.
50. F. Jager, S. Jager, O. Krutle, N. Friedman, M. Sheves, K. P. Hofmann and F. Siebert, Interactions of the beta-ionone ring with the protein in the visual pigment rhodopsin control the activation mechanism. An FTIR and fluorescence study on artificial vertebrate rhodopsins, *Biochemistry*, 1994, **33**, 7389-7397.
51. R. Vogel, F. Siebert, S. Ludeke, A. Hirshfeld and M. Sheves, Agonists and partial agonists of rhodopsin: retinals with ring modifications, *Biochemistry*, 2005, **44**, 11684-11699.
52. F. J. Bartl, O. Fritze, E. Ritter, R. Herrmann, V. Kuksa, K. Palczewski, K. P. Hofmann and O. P. Ernst, Partial agonism in a G Protein-coupled receptor: role of the retinal ring structure in rhodopsin activation, *J. Biol. Chem.*, 2005, **280**, 34259-34267.
53. R. Vogel, S. Ludeke, F. Siebert, T. P. Sakmar, A. Hirshfeld and M. Sheves, Agonists and partial agonists of rhodopsin: retinal polyene methylation affects receptor activation, *Biochemistry*, 2006, **45**, 1640-1652.
54. R. Vogel, G. B. Fan, M. Sheves and F. Siebert, The molecular origin of the inhibition of transducin activation in rhodopsin lacking the 9-methyl group of the retinal chromophore: a UV-Vis and FTIR spectroscopic study, *Biochemistry*, 2000, **39**, 8895-8908.
55. C. K. Meyer, M. Bohme, A. Ockenfels, W. Gartner, K. P. Hofmann and O. P. Ernst, Signaling states of rhodopsin. Retinal provides a scaffold for activating proton transfer switches, *J. Biol. Chem.*, 2000, **275**, 19713-19718.
56. B. Knierim, K. P. Hofmann, W. Gartner, W. L. Hubbell and O. P. Ernst, Rhodopsin and 9-demethyl-retinal analog: effect of a partial agonist on displacement of transmembrane helix 6 in class A G protein-coupled receptors, *J. Biol. Chem.*, 2008, **283**, 4967-4974.
57. K. Boesze-Battaglia and A. D. Albert, Phospholipid distribution among bovine rod outer segment plasma membrane and disk membranes, *Exp. Eye Res.*, 1992, **54**, 821-823.
58. K. Boesze-Battaglia and A. D. Albert, Fatty acid composition of bovine rod outer segment plasma membrane, *Exp. Eye Res.*, 1989, **49**, 699-701.
59. A. D. Albert and K. Boesze-Battaglia, The role of cholesterol in rod outer segment membranes, *Prog. Lipid Res.*, 2005, **44**, 99-124.
60. O. Soubias and K. Gawrisch, The role of the lipid matrix for structure and function of the GPCR rhodopsin, *Biochim. Biophys. Acta.*, 2012, **1818**, 234-240.
61. O. Soubias, W. E. Teague, Jr., K. G. Hines, D. C. Mitchell and K. Gawrisch, Contribution of membrane elastic energy to rhodopsin function, *Biophys. J.*, 2010, **99**, 817-824.
62. D. C. Mitchell, M. Straume, J. L. Miller and B. J. Litman, Modulation of metarhodopsin formation by cholesterol-induced ordering of bilayer lipids, *Biochemistry*, 1990, **29**, 9143-9149.
63. S. L. Niu, D. C. Mitchell and B. J. Litman, Manipulation of cholesterol levels in rod disk membranes by methyl-beta-cyclodextrin: effects on receptor activation, *J. Biol. Chem.*, 2002, **277**, 20139-20145.
64. M. Straume and B. J. Litman, Equilibrium and dynamic bilayer structural properties of unsaturated acyl chain phosphatidylcholine-cholesterol-rhodopsin recombinant vesicles and rod outer segment disk membranes as determined from higher order analysis of fluorescence anisotropy decay, *Biochemistry*, 1988, **27**, 7723-7733.

65. A. D. Albert, J. E. Young and P. L. Yeagle, Rhodopsin-cholesterol interactions in bovine rod outer segment disk membranes, *Biochim. Biophys. Acta.*, 1996, **1285**, 47-55.
66. G. Khelashvili, A. Grossfield, S. E. Feller, M. C. Pitman and H. Weinstein, Structural and dynamic effects of cholesterol at preferred sites of interaction with rhodopsin identified from microsecond length molecular dynamics simulations, *Proteins*, 2009, **76**, 403-417.
67. M. Jafurulla, S. Tiwari and A. Chattopadhyay, Identification of cholesterol recognition amino acid consensus (CRAC) motif in G-protein coupled receptors, *Biochem. Biophys. Res. Commun.*, 2011, **404**, 569-573.
68. M. A. Hanson, V. Cherezov, M. T. Griffith, C. B. Roth, V. P. Jaakola, E. Y. Chien, J. Velasquez, P. Kuhn and R. C. Stevens, A specific cholesterol binding site is established by the 2.8 A structure of the human beta2-adrenergic receptor, *Structure*, 2008, **16**, 897-905.
69. J. Oates and A. Watts, Uncovering the intimate relationship between lipids, cholesterol and GPCR activation, *Curr. Opin. Struct. Biol.*, 2011, **21**, 802-807.
70. M. F. Brown, Curvature forces in membrane lipid-protein interactions, *Biochemistry*, 2012, **51**, 9782-9795.
71. M. Beck, F. Siebert and T. P. Sakmar, Evidence for the specific interaction of a lipid molecule with rhodopsin which is altered in the transition to the active state metarhodopsin II, *FEBS Lett.*, 1998, **436**, 304-308.
72. N. R. Civjan, T. H. Bayburt, M. A. Schuler and S. G. Sligar, Direct solubilization of heterologously expressed membrane proteins by incorporation into nanoscale lipid bilayers, *Biotechniques*, 2003, **35**, 556-560, 562-553.
73. T. H. Bayburt, A. J. Leitz, G. Xie, D. D. Oprian and S. G. Sligar, Transducin activation by nanoscale lipid bilayers containing one and two rhodopsins, *J. Biol. Chem.*, 2007, **282**, 14875-14881.
74. T. H. Bayburt, S. A. Vishnivetskiy, M. A. McLean, T. Morizumi, C. C. Huang, J. J. Tesmer, O. P. Ernst, S. G. Sligar and V. V. Gurevich, Monomeric rhodopsin is sufficient for normal rhodopsin kinase (GRK1) phosphorylation and arrestin-1 binding, *J. Biol. Chem.*, 2011, **286**, 1420-1428.
75. H. Tsukamoto, A. Sinha, M. DeWitt and D. L. Farrens, Monomeric rhodopsin is the minimal functional unit required for arrestin binding, *J. Mol. Biol.*, 2010, **399**, 501-511.
76. S. Banerjee, T. Huber and T. P. Sakmar, Rapid incorporation of functional rhodopsin into nanoscale apolipoprotein bound bilayer (NABB) particles, *J. Mol. Biol.*, 2008, **377**, 1067-1081.
77. A. M. D'Antona, G. Xie, S. G. Sligar and D. D. Oprian, Assembly of an activated rhodopsin-transducin complex in nanoscale lipid bilayers, *Biochemistry*, 2014, **53**, 127-134.
78. K. Kojima, Y. Imamoto, R. Maeda, T. Yamashita and Y. Shichida, Rod visual pigment optimizes active state to achieve efficient G protein activation as compared with cone visual pigments, *J. Biol. Chem.*, 2014, **289**, 5061-5073.
79. P. Stepien, A. Polit and A. Wisniewska-Becker, Comparative EPR studies on lipid bilayer properties in nanodiscs and liposomes, *Biochim. Biophys. Acta.*, 2015, **1848**, 60-66.
80. A. K. Kusnetzow, C. Altenbach and W. L. Hubbell, Conformational states and dynamics of rhodopsin in micelles and bilayers, *Biochemistry*, 2006, **45**, 5538-5550.
81. D. Marsh, A. Watts, R. D. Pates, R. Uhl, P. F. Knowles and M. Esmann, ESR spin-label studies of lipid-protein interactions in membranes, *Biophys. J.*, 1982, **37**, 265-274.
82. A. Watts, I. D. Volotovski and D. Marsh, Rhodopsin-lipid associations in bovine rod outer segment membranes. Identification of immobilized lipid by spin-labels, *Biochemistry*, 1979, **18**, 5006-5013.
83. D. Marsh, Electron spin resonance in membrane research: protein-lipid interactions from challenging beginnings to state of the art, *Eur. Biophys. J.*, 2010, **39**, 513-525.